Sciences at Ca' Foscari

# Distribution of nanosilica dispersions in Lecce stone

Laura Falchi, Eleonora Balliana, Francesca Caterina Izzo,
Laura Agostinetto, Elisabetta Zendri

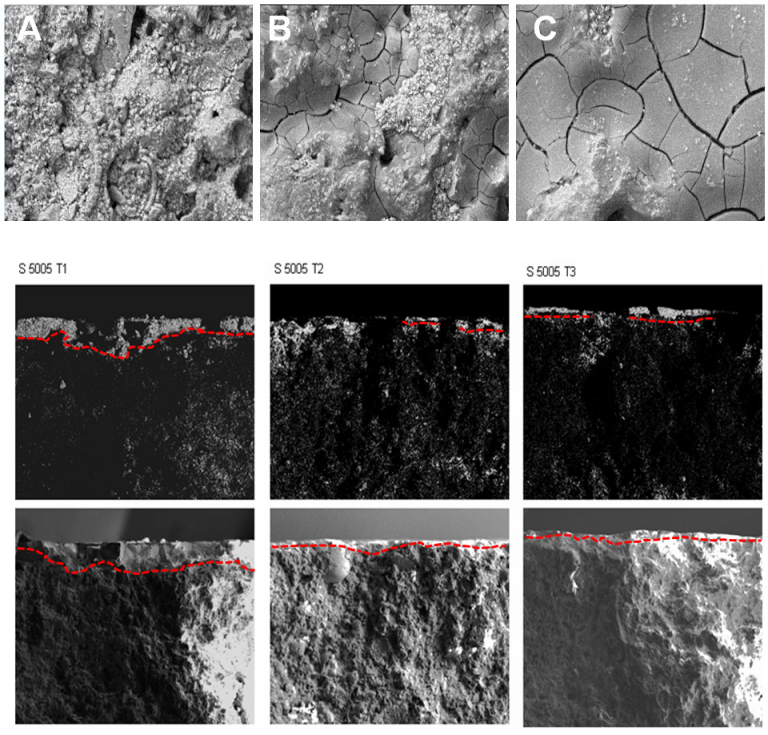


***Lecce stone treated with different nanosilica dispersion: surface SEM immages and EDX Si elemental mapping***

Edizioni
Ca'Foscari

# Distribution of nanosilica dispersions in Lecce stone

*Laura Falchi[b*], Eleonora Balliana[a*], Francesca Caterina Izzo[a*], Laura Agostinetto[a], Elisabetta Zendri[a*]*

[a] Department of Molecular Sciences and Nanosystems, Ca' Foscari, University of Venice, Dorsoduro 2137, 30123 Venezia, Italy.
[b] Department of Environmental Sciences, Informatics and Statistic, Ca' Foscari, University of Venice, Via Torino 155B, 30170 Mestre, Venezia, Italy.
* e-mails: laura.falchi@stud.unive.it, elizen@unive.it

Received: 2013-03-11
Accepted: 2013-04-26

**Abstract:** The aim of the present work is to study the application of four water-based nanosilica dispersions on carbonate rocks in terms of penetration depth, particle dimensions, physical-chemical characteristics and stone pore radius distribution. Preliminary investigations of untreated Lecce stone and nanosilica dispersions were performed considering different chemical-physical parameters (e.g. porosity, viscosity, surface tension, pH, zeta potential) and combining them with TEM observations. Different treatments of Lecce stone were then tested and investigated by SEM- EDX microscopy. In particular, silicon elemental mapping and its distribution profiles were registered on samples with EDX technique for understanding the relation between the dispersion and the stone. Despite the low viscosity and small dimensions of the nanosilica particles, the products seemed unable to deeply penetrate in the porous substrate. However, modification of the surface tension of the dispersions might improve the transport within the stone of the nanodispersions.

**Keywords:** Nanosilica, Consolidation, Zeta-potential, SEM-EDX, Lecce Stone, Colloids.

DOI: 10.7361/SciCF-441

### *1. Introduction*

In the last decades, thanks to the growing interest for the preservation and maintenance of architectural surfaces, significant progresses has been made in understanding the factors and the mechanisms responsible for materials decay and in developing suitable guidelines for their conservation [1-4]. In particular, the consolidation of porous stones, often necessary when materials are seriously damaged by decohesion and disaggregation, has been investigated/analysed in several researches and studies [4-9].

Most of the recent studies on new stone consolidants led to the development of nanotechnology products, first of all colloidal nanodispersions [9-12], e.g. calcium hydroxide dispersions. Alcohol-based nanodispersions of calcium and magnesium hydroxide and carbonate have in fact been successfully used for the consolidation and restoration of *frescoes* and mural paintings [13-16]. Beside nanolime dispersions, another kind of consolidant might be aqueous colloidal nanosilica, characterised by the better eco friendly solvent, i.e. water, and the most used strengthening agent, i.e. silica [17].

The use of aqueous dispersions and nanosized silica particles would represent a valuable alternative to the traditional solvent-based products. Nanosized silica particles might be able to deeply penetrate the substrate and to form a network of silica xerogel compatible with inorganic matrices as stone. However, different aspects regarding the interactions between nanosilica dispersions and porous stone substrate, and the transport mechanism have been little investigated and are not well-known yet. Many of the published studies focused in fact on the transport of nanodispersions inside soils and granular matrices [18-22], but complete theoretical models are not yet available for porous stone. In general, the penetration of a dispersion inside a porous material is influenced by the characteristics of the dispersion itself and the material, and the physical-chemical and electrostatic interactions between them [23]. Recent studies [24-26] pointed out how colloids

transport inside a porous matrix exponentially decrease with the travel distance of the wetting front and the deposition of colloids particles into the matrix. Surfactants (e.g. alcohols, humic substances, aliphatics and commercial surfactants) are able to reduce the surface tension modifying the retention, the transport and the remobilisation of the colloids. The reduction of the surface tension can in fact decrease the capillary pressure in unsaturated porous media and enhance therefore the drainage.

The aim of the present work is to analyse the behaviour of four commercial water-based silica dispersions used as consolidants for carbonate rock, focusing in particular on particle dimensions, physical-chemical characteristics and penetration depth of the colloidal dispersions in relation to the substrate.

## 2. Materials and Methods

### *2.1. Chemical-physical characterisation of the nanosilica dispersions*

Four commercial water-based colloidal silicas with different average radius were selected as possible consolidants for porous stone: Dispercol S5005, S4510, S4020, S3030 (Bayer®). The products were dispersed in water at 20% (dry weight of the colloid).

All dispersions were observed by TEM microscopy (JEOL TEM 3010) to evaluate the shape and the radius of the nanoparticles. Moreover , the pH (744 pH Meter Metrohm), the density (following the UNI EN ISO 2811-1 2003), and the viscosity (using a rotational rheometer AR G2 TA Instruments, stepped flow mode) of each dispersions were measured. A small amount of the dispersions were also dried at room temperature (20°C and 60% relative humidity) to constant weight. The obtained Xerogels were then characterised using: FT-IR analysis on KBr pellets in the 4000-400 $cm^{-1}$ region (Nicolet magna IR750 spectrometer); XRD diffraction (Philips DW320 diffractometer); BET Surface area measurement (Micrometrics ASAP 2010 surface area analyser at 77 Kelvin for pressure between 0,05 and 0,3 $p/p_0$ with Nitrogen as adsorbing gas).

### *2.2. Chemical-physical characterisation of stone substrate*

The dispersions were applied on Lecce stone, a limestone commonly used for the construction and decoration of historic buildings in southern Italy. This stone is characterised by a gold yellow colour and a rather high total porosity (around 36%) [27]. The total open porosity of the Lecce stone was obtained by mercury intrusion porosimetry (Pascal 240 ThermoQuest porosimeter) and its microstructure was observed by SEM-EDX (JEOL JSM-5600 LV).

### *2.3. Evaluation of the interactions between Lecce stone and the dispersions*

The interaction between the dispersions and the Lecce stone was investigated considering the wettability of the substrate and the surface tension of the dispersions. Moreover, the chemical potential of the substrate and of the dispersion S4020, considered as more significant, were analysed as well.

The wettability of the substrate was obtained measuring the contact angle between stone-water and the contact angle between stone-liquid dispersions.

The surface tension of the dispersions was determined by the pendant drop mode ("FTA 1000 C class", First Ten Ångstrom Instruments) analysing the shape of pendant drops of the dispersions. At the hydrodynamic equilibrium between the pendant drop and the surrounding air , the profile of the drops is in fact strongly related to the surface tension as reported by Bashforth and Adams equation [28].

The zeta potential measurements of Lecce stone were performed with a Zeta CAD (CAD Instruments France) equipped with a special cell for tangential measurements [29]. This apparatus measures the electrical potential difference generated by the imposed movement of an electrolyte solution through a thin slit channel between a couple of 1mm high Lecce stone slices. A data file is created by recording the streaming potential and the corresponding differential pressure across the plug versus time.

The zeta potential analysis of the dispersion Dispercol S 4020 was obtained with a DT1200 Dispersion Technology acoustic spectrometer. The zeta potential is determined measuring the interaction between the electric and the acoustic field applied to the dispersion [30]. During the measurements, automate titration is carried out for monitoring possible agglomeration in the dispersion due to change in the pH.

### *2.4. Treatments of the stone samples and study of the distribution of the dispersions*

The four selected colloids were applied at 20% dry weight concentration by percolation on 2×2×1 cm Lecce stone specimens. Three different application methods were applied each on 5 different stone samples:

- Treatment 1(T1)-the dispersions were applied by percolation on the stone surface covered with Japanese paper[1].
- Treatment 2 (T2)-the stone was first impregnated by ethanol, for modifying the surface tension, and then treated with the dispersions. The stone surface was covered with Japanese paper.
- Treatment 3 (T3)- the dispersions, after acidification to pH 8 with HCl 0,5 M, were applied to the stone samples[2].

Once treated, the samples were dried at room temperature for 20 days to constant weight and the final dry weight of the penetrated products was calculated. The morphology and the distribution of the deposited phases were studied on the surfaces and on the cross sections of the stone samples by optical microscopy and SEM-EDX analysis (Jeol JSM-5600 LV). The cross sections were not smoothed in order to maintain the distribution of the products therein. Elements mapping distribution and concentration profile were obtained by punctual measurement with EDX probe; for the concentration profile an average of ten measurements every 100 micron was considered.

## *3. Results and discussion*

### *3.1. Chemical-physical characteristics of the dispersions*

Table 1 summarizes the characteristics of the dispersions. The diameter data are the one reported on the technical data sheets.

Table 1. Characteristics of the dispersions.

| Name | Diameter nm | Dryweight % | pH | Density g/cm$^3$ | Viscosity mPa·s | Surface Tension dy/cm |
|---|---|---|---|---|---|---|
| S 5005 | 55 | 52 | 9.9 | 1.38 | 1.23 | 61.9 |
| S 4510 | 30 | 48 | 10.1 | 1.34 | 1.22 | 67.8 |
| S 4020 | 15 | 43 | 10.5 | 1.29 | 1.28 | 67.9 |
| S 3030 | 9 | 34 | 10.1 | 1.21 | 1.33 | 65.8 |

All the dispersions are characterised by a low viscosity and a surface tension comparable to deionised water (72 dy/cm). The pH of the dispersions is around 10 and related to the presence of sodium hydroxide added as a stabiliser by the manufacturer.

TEM images of the colloidal silica (Fig.1) show a regular spherical shape of the nanoparticles with different average diameters. Interesting is the case of the S5005 nanoparticle dispersion where the nanoparticles have an average diameter value around 100 nm, greater than the one declared by the technical data sheets (55nm).

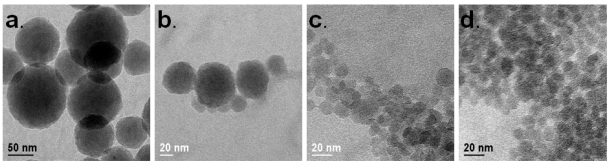


Figure 1. Tem Images: a-S5005, b- S4510, c- S4020, d-S3030.

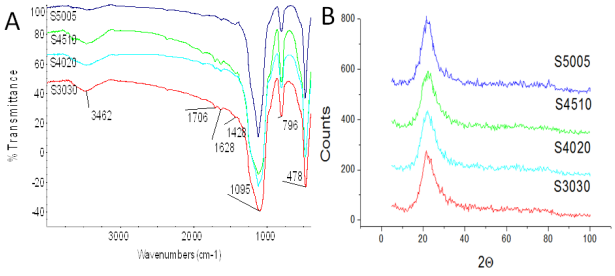


Figure 2a. FT-IR spectra of the nanosilica xerogels, from the top: S5005, S4510, S4020, S3030. Figura 2b. XRD spectra of the nanosilica xerogels.

The FT-IR spectra of the Xerogels obtained from the dried dispersions (Fig. 2.A) show the typical absorbance bands associated to amorphous silica, in particular the 470 cm$^{-1}$ bending peak and the 800 cm$^{-1}$ and 1110 cm$^{-1}$ stretching peaks of the Si-O-Si

1 Japanese or Washi paper is a paper made from the bark of Kozo, rice, bamboo, or wheat. It is a strong, not acid, translucent paper, widely used in conservation practice thanks to its high strength and its malleability. In this work a rice Japanese paper of 10g/m$^2$ was used for prolonging the contact time between the dispersion and the stone and obtaining a more homogeneous distribution of the products.

2 The changes in pH should modify the zeta potential of dispersions and lead to a better interaction with the stone matrix and product penetration.

are visible. The small 1428 $cm^{-1}$ peak, slightly visible in S5005 and S3030 spectra, denotes the presence of sodium carbonate probably linked to a partial carbonation of the sodium hydroxide present in the dispersion as stabilising agent.

XRD diffraction patterns of dried products have highlighted the formation of a xerogel consisting of amorphous silica (Fig. 2.B), confirmed by a broad peak at about 20 2θ.

Table 2 reports the values of the specific surface area of the xerogels obtained by BET analysis. The values are strongly related to the nanoparticles diameters and there is an inverse proportion between the area and the dimension of the nanoparticles radius. The area values in fact increase when the nanoparticles radius decreases.

Table 2. Surface area and porosity data obtained by BET analysis.

| Name | ø(nm) | Surface area ($m^2/g$) | Total volume porosity ($cm^3/g$) |
|---|---|---|---|
| S 5005 | 55 | 41 | 0.19 |
| S4510 | 30 | 74 | 0.17 |
| S4020 | 15 | 128 | 0.22 |
| S3030 | 9 | 190 | 0.24 |

### *3.2. Porosity of the substrate*

Based on the MIP measurements (Fig. 3 and Table 3) Lecce stone is characterised by a high total open porosity (approximately 40%), and a bimodal distribution of pores diameter with a high percentage of pores having diameters near 0,5 μm or 5 μm.

Table 3. Results of MIP analysis.

| | |
|---|---|
| Total cumulative volume (cc/g) | 0.23±0.10 |
| Average pore radius (Micron) | 2.30±0.84 |
| Total porosity (%) | 38.7±1.58 |
| Bulk density (g/cm3) | 1.65±0.01 |

### *3.3. Wettability of the substrate*

The wettability of the stone was determined measuring the contact angles of sessile drops formed by deionised water and different products on Lecce stone. Once spread on the surface, the liquids were easily absorbed by the stone in few seconds with contact angles always equivalent to zero. The stone resulted completely wettable by water and by the dispersions.

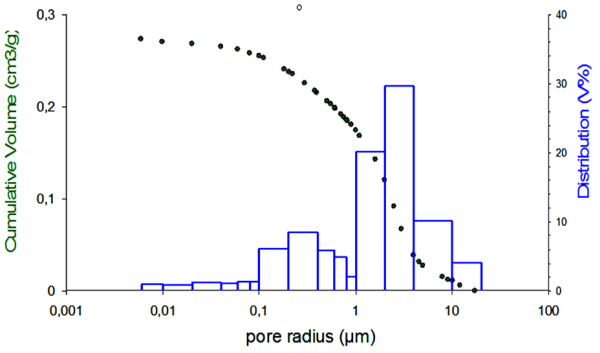


Figure 3. Distribution of pore radius versus cumulative volume in Lecce Stone

### *3.4. Zeta potential (ζ) measurements*

The zeta potential (ζ) of Lecce stone was determined by recording the streaming potential and the corresponding differential pressure. Despite the difficulties to establish a stable regime within the measuring cell, due to the roughness and the porosity of the sample surface, a zeta potential of -14mV was calculated from the corresponding streaming potential of -0.0625 mV/mBar. The zeta potential can be calculated, knowing the corresponding electrical conductivity (0,158 mS/cm) at measuring temperature (19.5°C), as established by Yaroshchuk and Ribitisch [29]. Moreover, for testing how the variation of pH affects the surface exchanges, a test was developed adding KOH to the electrolyte solution (Table 4).

Table 4: ζ measurements of Lecce stone and S4020

| Lecce Stone | | S4020 | |
|---|---|---|---|
| pH | ζ (mV) | pH | ζ (mV) |
| 6.9 | -14 | 6.81 | -11.07 |
| 8.3 | -19.7 | 8.21 | -23.70 |
| 11 | -44 | 10,24 | -42.12 |

Based on the experimental data, there is an inverse relation between the pH and the zeta potential. In the case of the Lecce stone, increasing values of pH correspond to decreasing zeta potential values reaching -44mV, when the pH of the electrolytes liquid is around 11. Higher values of zeta potential correspond to a thicker electrical double layer which can interact with other charged particles. The pH values of the dispersions used in these studies were

pH around 9-10. The surface of the stone at this pH is characterised by a higher zeta potential and consequently by a thicker electric double layer that can interact with the nanoparticles repulsing them.

The zeta potential of one of the dispersion S4020 was also determined at different pH obtained by adding HCl to the dispersion (Table 4 and Fig. 4.). The zeta potential of Dispercol S4020 decreased with the increasing of pH, confirming moreover the relation between the two parameters.

The zeta potential of the original dispersion (pH 10-11) was around -40 mV, which corresponds to a stable dispersion [30]. At -40mV of zeta potential, the nanoparticles repulsed each other, but could also play a repulsion force against the surface of the stone limiting therefore the penetration.

Decreasing value of the pH often corresponded to higher value of the zeta potential due to lower repulsive forces. A slight change in the pH of the dispersions could therefore facilitate a deeper penetration of dispersions inside the stones. A pH at about 7-7.5, corresponding to a potential close to 25 mV, has to be considered however the limit due to the tendency of the dispersion to flocculate.

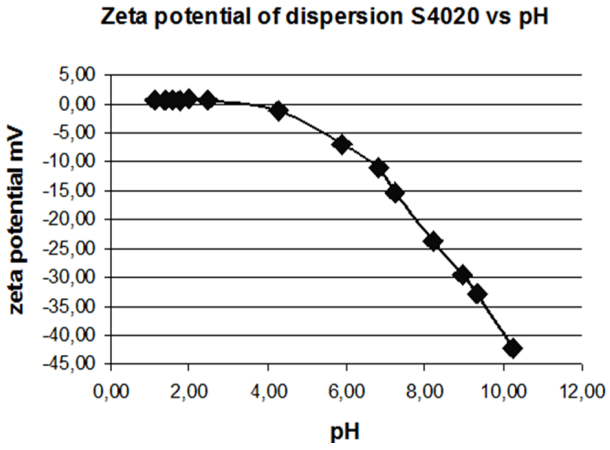


Figure 4. Zeta potential measurement versus pH for the dispersion S4020.

### *3.5. Treatments and distribution of the dispersions inside the stone*

The percentage of product absorbed during each treatment (T1,T2,T3) was measured as weight variation of the stone before and after application and listed in Table 5.

Table 5. amount of products penetrated.

| Name | ø(nm) | Weight variation after treatments DP% | | |
|---|---|---|---|---|
| | | T1 | T2-ethanol | T3- pH 8 |
| S 5005 20%w | 55 | 0.5±0.1 | 0.3±0.1 | 1.1±0.1 |
| S4510 20%w | 30 | 1±0.1 | 0.2±0.1 | 0.8±0.1 |
| S4020 20%w | 15 | 0.9±0.1 | 0.4±0.1 | 0.9±0.1 |
| S3030 20% w | 9 | 0.7±0.1 | 0.4±0.1 | 0.8±0.1 |

The amount of products penetrated was in any case higher than 1% respect the initial weight of the stone specimens.

All the dispersions showed the tendency to solidify on the surface forming a layer of xerogel, as shown in Fig. 5 referred to the treatment T1 here reported as an example. This tendency increased when using dispersions with lager nanoparticles size.

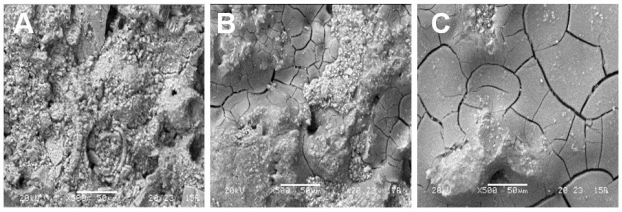


Figure 5. SEM images 500X of Lecce stone surface: A-not treated, B- 5050 20%, C -4020 20%.

Due probably to the porosity and structure of Lecce stone, the nanoparticles distributions were highly irregular. Despite the difficulties to estimate and exactly understand the penetration depth reached by the products, it was possible to notice some common tendencies between the different dispersions. The penetration depth (see distribution profile Fig.6 and EDX silicon maps Fig. 8-9) was limited at best to the first 2.5 mm in case of treatment with S5005 and S 4510 and to 1-1.5 mm when S4020 and S3030 were used. For all the tested treatments, while going deeper into the samples, the percentage of silicon quickly decreased to 0.5% ca which is the average value of Si in the untreated stone. The distribution profiles of S4020 and S3030 (Fig. 6) showed similar trends for the four different treatments in terms of penetration, being T2 only slightly better than the others.

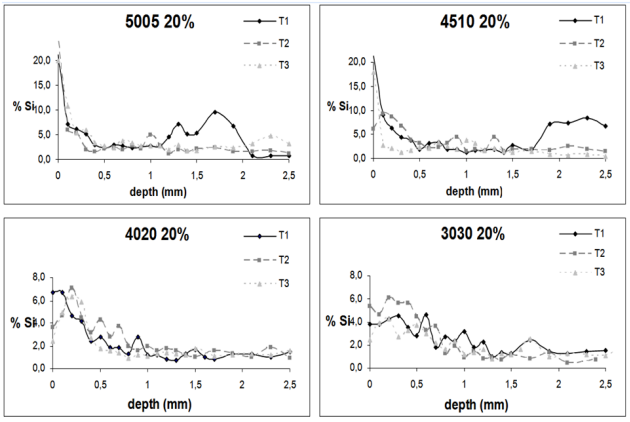


Figure 6. Distribution profiles of Si obtained through EDX standard less technique.

Peculiar is the distribution profiles of S5005 and S4510 (Fig. 6). When applied per percolation on Japanese paper (T1), the distribution profiles are irregular with a decrease percentage of Si in the first millimetre and an increase value in the second millimetre. The increasing concentration of Si is probably associated to the product distribution inside the stone open porosity. The silicon distribution profiles become more regular when applied with ethanol (T2) with a lower percentage of Si in the first layers and a more regular distribution inside the stone, while the third treatment (T3) did not present a good penetration depth. Distribution profiles of S4020 and S3030 (displayed in Fig. 6) show similar trends for the different treatments, with only treatment T2 slightly better than the other ones.

Fig.s 7, 8 and 9 report the SEM images and the associated elemental maps of Si in the cross sections of the untreated and treated samples. Fig. 8 clearly shows how nanoparticles with higher diameter (e.g. S5005) tend to form a thick layer of xerogel on the surface of the stone. The thickness of this layer is, however, significantly reduced when the dispersion was applied on stone samples pre-treated with ethanol as in treatment T2.

A slight variation to pH 8 of dispersions S5005 and S4510 did not avoid the formation of a xerogel layer on the surface. Dispersions with smaller nanoparticles (S4020 and S3030) did not form xerogel layers on the surface resulting in a more regular distribution of the product inside the stones. Observing the elemental maps of S4020 (Fig. 9) it is possible to see how T2 and T3 led to a good penetration depth.

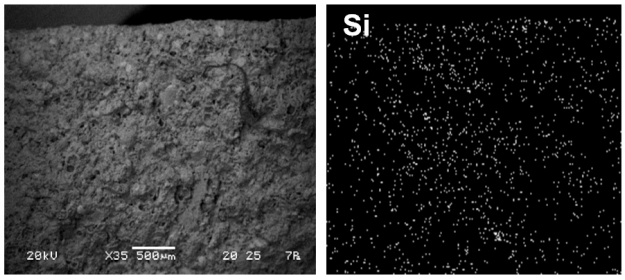


Figure 7. Si Kα elemental maps and SEM images of Lecce stone cross section.

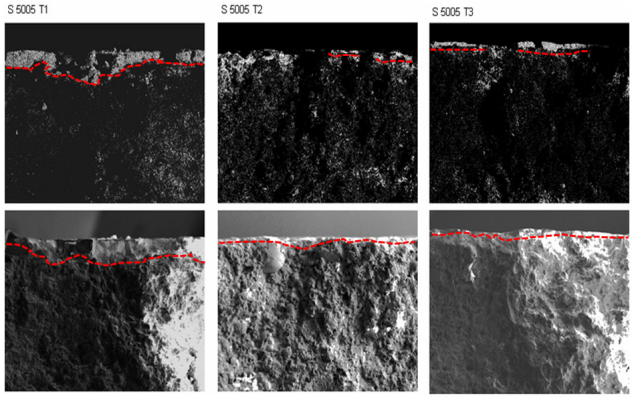


Figure 8. Si Kα elemental maps and SEM images of Lecce stone cross section after treatments with S5005 (ø 55nm): treatment 1 T1, treatment 2 T2, treatment 3 T3. The dotted line indicates the layer of xerogel deposited on the stone surfaces.

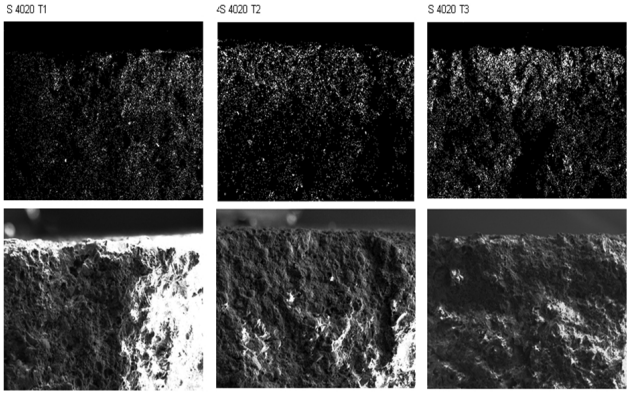


Figure 9. Si Kα elemental maps and SEM images of Lecce stone cross section after treatments with S4020 (ø 15 nm): treatment 1 T1, treatment 2 T2, treatment 3 T3.

### *4. Conclusions*

The penetration depth of a dispersion into a porous substrate is considered to be a function of the chemical-physical and electrostatic interaction between the substrate and the dispersion. Starting from this statement, different parameters of Lecce stone and nanosilica dispersions (such as surface tension, viscosity of the dispersion, porosity of the stone, chemical potential) were measured. Based on the obtained results, it was observed that:

- despite the little size of the particles (max 55 nm) in comparison to the average diameters of Lecce stone pore (about 0.5 µm and 5 µm), the dispersions were unable to deeply penetrate into the stone, but they arrested in the first 2 mm;
- the dispersions showed the tendency to form a xerogel layer on the surface of the samples, whereas the aqueous medium penetrated inside the stone;
- a pre-treatment of the stone surface with ethanol reduced the stone surface tension resulting in a better penetration of the dispersion;
- pH changes of the dispersions increased the zeta potential but did not give any real improvements in the penetration depth for dispersions with higher nanoparticles diameters; better results were observed for nanosilica with lower diameters.

Concluding, the modification of the stone surface tension (e.g. by using ethanol) could help in developing or optimizing the penetration of the products in the porous substrates obtaining a better consolidation effect.

Further studies with silica-based consolidants coformulated with surfactants might be considered in force of the compatibility of new dispersions and products with architectural and cultural surfaces.

### *5. Acknowledgments*

The authors thank MS. Davide Cristofori and MS. Martina Marchiori (Department of Molecular Sciences and Nanosystems, Ca' Foscari, University of Venice) for TEM and BET analyses.

### *6. References*

[1] *Recommendations for the Analysis, Conservation and Structural Restoration of Architectural Heritage*, ICOMOS, International Scientific Committee for Analysis and Restoration of Structures of Architectural Heritage, Document approved in the committee meeting in Barcelona the 15th June **2005**.

[2] E. Hansen et al., *Reviews in Conservation* **2003**, *4*, 13-25.

[3] I. Karatasios et al., *Constr Build Mater* **2009**, *23*, 2803-2812.

[4] G. Torraca, *Treatment of stone in monuments, A review of Principles and Processes*, in *Conservation of Stone I, Proceeding of the international Symposium*, Bologna **1995**, 297-315.

[5] J. Ciabach, *Investigation of the cross-linking of thermoplastic resins affected by ultraviolet radiation*, in J.O. Tate, N.H. Tennent and J.H. Townsend (eds.), *Proceedings of the symposium Resin in Conservation*, Scottish Society for Conservation and Restoration, Edinburgh, **1983**, 51-58.

[6] P. Maravelaki-kalaitzaki et al., *Prog. Org. Coat.* **2008**, *62*, 49-60.

[7] I. Nardini et al., *Influence of the application methodologies on the distribution of consolidant products within a porous material*, in LINEC (ed.), *Proceedings of the International Symposium Stone consolidation in cultural heritage, research and practice*, Lisbon, **2008**, 151-158.

[8] E. Zendri et al., *Indagini sulle variazioni microstrutturali di una pietra porosa trattata con consolidanti di diversa natura*, in G. Biscontin, G. Driussi (eds.), *Scienze e Beni Culturali* **2007**, *XXIII*, 607-615.

[9] P. Lopez-Arce et al., *Mater. Charact.* **2010**, *61*, 168-184.

[10] B. Simionescu, *Constr. Build. Mater,* **2009**, *23*, 3426-3430.

[11] P. Baglioni, R. Giorgi, *Soft Matter.* **2006**, *2*, 293-303.

[12] M.J. Mosquera et. al., *Langmuir* **2008**, *24*, 2772-2778.

[13] M. Drdacky et al., *J. Nano Res.* **2009**, *8*, 13-22.

[14] L. Dei, B. Salvadori, *J. Cult. Herit.* **2006**, *7*, 110-115.

[15] C. Rodriguez-Navarro et al., *Nanostructure and Irreversible Colloidal Behaviour of* $Ca(OH)_2$*: Implications in Cultural Heritage Conservation*, *Langmuir* **2005**, *21*, 10948-10957.

[16] E. Doehne, C.A. Price, *Stone Conservation, An Overview of Current Research*, 2nd edition, Canada Getty editions **2010**, 40-50.

[17] E. Zendri et al., *Con. Build. Mat.* **2006**, *10*, 1016.

[18] A.J. Pelley, N. Tufenkji, *J. Colloid. Interf. Sci.* **2008**, *321*, 74-83.

[19] J. Zhuang et al., *Water Res.* **2010**, *12*, 0-12.

[20] A. Scott et al., *Environ. Sci. Technol.* **2009**, *43*, 6996-7002.

[21] T. Baumann et al., *Water Res.* **2009**, doi:10.1016/j.watres.2009.11.035.

[22] S. Bradford, S. Torkzaban, *Colloid transport and retention in unsaturated porous media: a review of interface-, collector-, and pore-scale processes and models*, *Vadose Zone J.* **2008**, *7*, doi:10.2136/vzj2007.0092.

[23] B. Derjaguin, L. Landau, *Acta Physico Chemica URSS*, **1941**, *14*, 633-643.

[24] R.E. Zartman, R.A. Bartsch, *Soil Sci.* **1990**, *149*, 52-55.

[25] R.C. Walker et al., *J. Contam. Hydrol.* **1998**, *34*, 31-46.

[26] E.J. Henry et al., *J. Contamin. Hydrol.*, **2002**, *56*, 247-270.

[27] S. Bugani, M. Camaiti et al., *X-ray-spectrom*, **2007**, *36,* 316-320.

[28] E.Y. Arashiro, N.R. Demarquette, *Material Res.* **1999**, *2 (1*).

[29] P. Fevet et al., *J. Membrane Sci.*, **2003**, *226,* 227-236.

[30] AS. Dukhin, P.J. Goetz, *Colloid Surface A.* **1998**, *144*, 49-58.